

# We are IntechOpen, the world's leading publisher of Open Access books Built by scientists, for scientists

6,900

Open access books available

186,000

International authors and editors

200M

Downloads

Our authors are among the

154

Countries delivered to

TOP 1%

most cited scientists

12.2%

Contributors from top 500 universities



WEB OF SCIENCE™

Selection of our books indexed in the Book Citation Index  
in Web of Science™ Core Collection (BKCI)

Interested in publishing with us?  
Contact [book.department@intechopen.com](mailto:book.department@intechopen.com)

Numbers displayed above are based on latest data collected.  
For more information visit [www.intechopen.com](http://www.intechopen.com)



---

# Mesoporous TiO<sub>2</sub> Thin Films: State of the Art

---

Francesca Scarpelli, Teresa F. Mastropietro,  
Teresa Poerio and Nicolas Godbert

Additional information is available at the end of the chapter

<http://dx.doi.org/10.5772/intechopen.74244>

---

## Abstract

Mesoporous TiO<sub>2</sub> thin films (MTTFs), thanks to their particularly high surface area, controlled porosity, high flexibility in composition, and surface design, are promising candidates in different application fields such as sensors, self-cleaning coatings, lithium-ion batteries (LIBs), photocatalysis, and new-generation solar cells. This chapter is focused on the synthetic and post-synthesis aspects that can affect the TiO<sub>2</sub> mesoporous structure and consequently the MTTF properties. In particular, after a brief summary of TiO<sub>2</sub> properties, all experimental conditions to prepare MTTFs are reviewed as well as the main characterization techniques employed to study their physicochemical and photocatalytic properties. An overview of the main applications of MTTFs is also proposed, mainly focused on the use of MTTFs in sensors and LIBs.

**Keywords:** mesoporous TiO<sub>2</sub> thin films, X-ray diffraction, anatase, rutile and brookite

---

## 1. Introduction

Crystalline mesoporous metal oxide materials are potential candidates for a number of applications, such as battery electrodes [1], fuel cells [2, 3], optoelectronic devices [4], photovoltaic devices [5], and photocatalysis [6], due to their variable oxidation states and unusual magnetic, electronic, and optical properties compared to silicates. In particular, titania-based mesoporous materials have been extensively investigated since titania is transparent in the visible region, nontoxically biocompatible, and photocorrosion-free and can be fabricated by relatively cheap methods. For these numerous properties, titania is employed for various applications in diverse scientific fields, ranging from self-cleaning coatings [7], lithium-ion batteries (LIBs) [8], photocatalysis [9], new-generation solar cells [10], and membrane [11]

---

to antibacterial applications [12]. However, to design efficient systems and devices for the above-cited uses, stable materials with a well-defined crystalline structure, highly controlled crystallite size and shape, as well as high available surface area and accessible pore networks able to ensure contact with catalytic substrates, polymers, or nanospecies are required [13]. Although the early mesoporous materials were produced in the form of powders, some applications, such as membranes, low-dielectric-constant interlayers, optical sensors, and optoelectronic devices, require ultralow-k dielectrics and low-refractive-index materials with a good mechanical stability and of hydrophobic nature. These requirements led to the preparation of mesoporous thin films [14–16]. After a brief description of the different  $\text{TiO}_2$  polymorphs and properties, the present chapter will therefore be dedicated to mesoporous  $\text{TiO}_2$  thin films (MTTFs), reviewing the different preparation methods reported throughout the literature, the main characterization techniques employed to study the structure and the morphology of the prepared thin films, and finally the description of their most successful applications.

## 2. Intrinsic properties of $\text{TiO}_2$

Titanium belongs to the IVA group of elements and, as many other metals, is able to form a wide range of oxides. Titanium(IV) dioxide (titania) exists in three common crystalline phases: rutile, which is the thermodynamically stable phase, and the metastable phases anatase and brookite. Anatase and rutile have more extensive applications because they are more stable than brookite (**Figure 1**). In all three forms, titanium ( $\text{Ti}^{4+}$ ) atoms are coordinated to six oxygen ( $\text{O}^{2-}$ ) atoms, forming “ $\text{TiO}_6$ ” octahedra. Anatase and rutile have a tetragonal

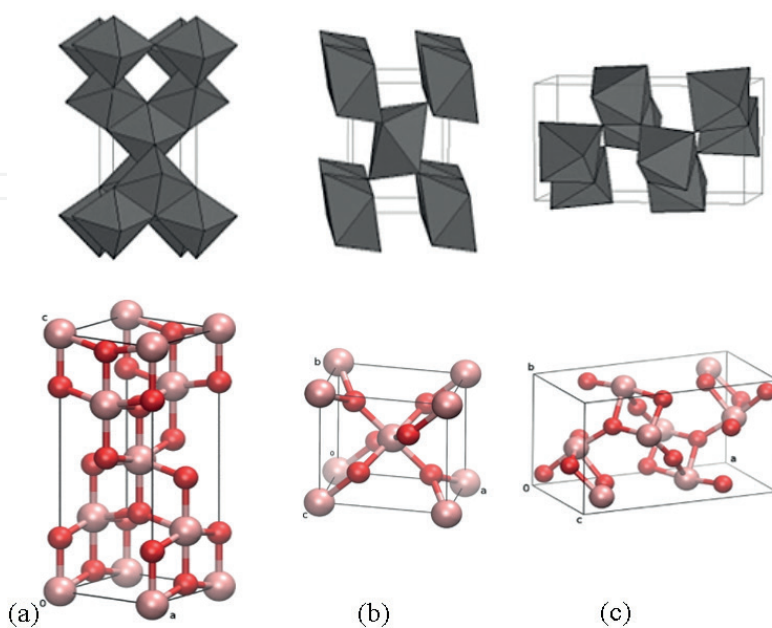


**Figure 1.** Crystal structures of  $\text{TiO}_2$ : (a) anatase, (b) rutile, and (c) brookite (adapted from Ref. [17]) (**Table 1**).

Property	TiO <sub>2</sub>		
Molecular weight (g mol <sup>-1</sup> )	79.88		
Melting point (°C)	1825		
Boiling point (°C)	2500–3000		
Property	Anatase	Rutile	Brookite
Refractive index [18]	2.52	2.72	2.63
Dielectric constant	31	114	
Crystal structure [19, 20]	Tetragonal	Tetragonal	Orthorhombic
Space group	<i>I4<sub>1</sub>/amd</i>	<i>P4<sub>2</sub>/mmm</i>	<i>Pbca</i>
Lattice constant (Å)	a = b = 3784 c = 9515	a = b = 4593 c = 2959	a = 9184 b = 5447 c = 5145
Molecule/cell	4	2	8
Volume (Å <sup>3</sup> )	136.25	62.07	257.38
Density (g cm <sup>3</sup> )	3.79	4.13	3.99

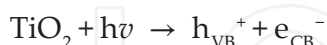
**Table 1.** Compared intrinsic properties of main TiO<sub>2</sub> polymorphs.

geometry, differently from brookite, which has an orthorhombic geometry. In rutile, the “TiO<sub>6</sub>” octahedron is slightly distorted, while anatase consists of strongly distorted octahedral units. In the rutile structure, each octahedron is surrounded by ten close octahedrons; instead, in the anatase polymorph, each octahedron is in contact with eight neighbors. Interatomic distances also differ between the polymorphs. For anatase, with respect to rutile, the Ti-Ti distances are lengthier and, instead, the Ti-O distances are shorter. These differences in lattice structures cause different mass densities and electronic band structures between the two forms of TiO<sub>2</sub>. Due to its intrinsic properties, the anatase phase is the most interesting one for applications.

Titania is an n-type semiconductor since, like other metal transition oxides, the oxygen vacancies represent the predominant defect type in TiO<sub>2</sub>. Indeed, every crystal has various structural defects; for example, point defects, which are empty sites (vacancies), where constituent atoms are missing within the structure and interstitial atoms occupy the space between the regular atomic sites. The point defects contribute to the electrical conductivity in two ways: they can provide ionization, and they can also move in response to an electric field producing an ionic current. An oxygen vacancy is formed by the transfer of an oxygen atom on a normal site to the gaseous state. These oxygen vacancies act as electron donors, so the material contains an excess of electrons resulting in an increase of the electrical conductivity.

TiO<sub>2</sub> exhibits photocatalytic oxidation (PCO) and photoinduced superhydrophilicity (PSH) when it is illuminated with UV light, making TiO<sub>2</sub> a good candidate for photocatalyst materials and self-cleaning surfaces in air.

The PCO property is activated by absorption of UV photons of energy greater than  $\text{TiO}_2$  bandgap energy. For anatase phase this energy is 3.2 eV; therefore, UV light ( $\lambda \leq 387$  nm) is required, while rutile phase has energy of 3.0 eV ( $\lambda = 400$  nm). The absorption of a photon excites an electron to the conduction band ( $e_{\text{CB}}^-$ ) generating a positive hole in the valence band ( $h_{\text{VB}}^+$ ), so that photoexcitation produces electron-hole pairs.



The charge carriers can migrate to the catalyst surface and initiate redox reactions with adsorbates. The redox potential for hole in VB is +2.53 V, which is sufficiently oxidizing to overcome the binding energy of electron in  $\text{OH}^-$  to form a hydroxyl radical from water. The hydroxyl radical can subsequently oxidize organic species with mineralization producing mineral salts,  $\text{CO}_2$ , and  $\text{H}_2\text{O}$ . Similarly, an electron in CB ( $E = -0.52$  V) is sufficiently reductive to react with  $\text{O}_2$  to form  $\text{O}_2^{\bullet-}$  (superoxide radical anion), which can react with  $\text{H}^+$  to produce hydroperoxide radical contributing to the degradation of organic molecules (**Figure 2**) [21]. The main drawback in the use of titania as photocatalyst is its high electron-hole recombination rate, but several methods to improve photocatalytic activity by promoting separation of the electron-hole pair have been developed, such as doping and heterojunction coupling.

The PSH property consists in the alteration of the  $\text{TiO}_2$  wettability under UV irradiation and in the formation of a highly hydrophilic surface state. One possible explanation of the PSH property is that electrons reduce Ti(IV) cation sites in Ti(III) and holes oxidize  $\text{O}^{2-}$  anions to molecular oxygen. The expulsion of  $\text{O}_2$  molecules creates surface vacancies on which water

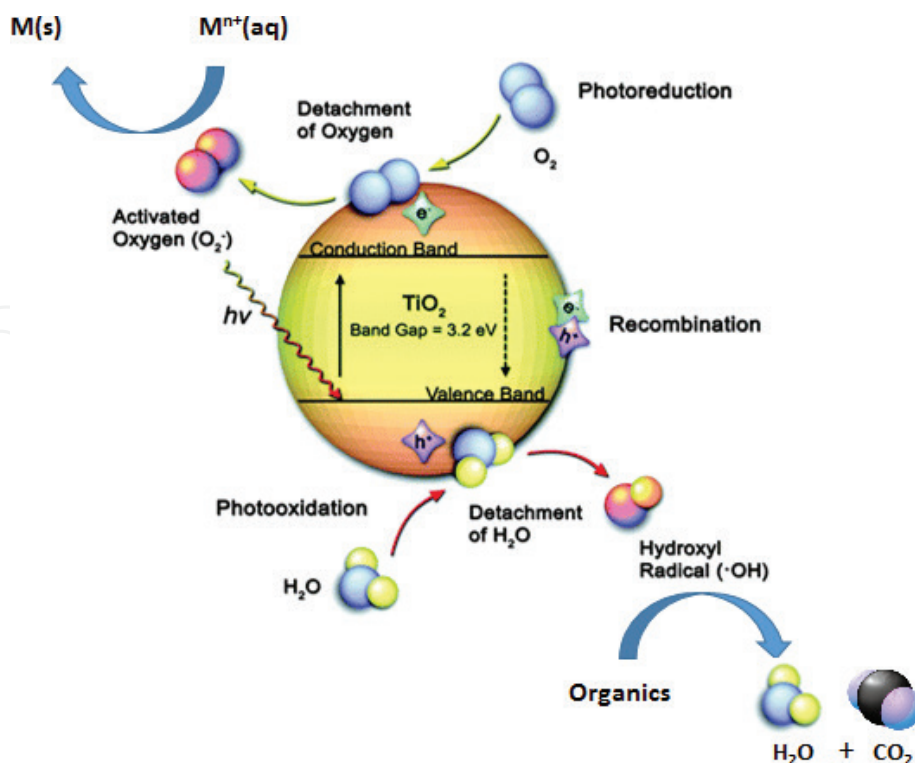


**Figure 2.** Schematic mechanism of  $\text{TiO}_2$  photoactivation (adapted from Ref. [22]).

can adsorb as OH groups, giving to the TiO<sub>2</sub> surface its superhydrophilic character. Indeed, when illuminated, titania surface exhibits amphiphilicity caused by the creation of alternating hydrophilic/hydrophobic domains. It was found that in the absence of UV illumination, the water contact angle for TiO<sub>2</sub> was *ca.* 72° (hydrophobic), while UV illumination turned it close to 1° (superhydrophilic) [23]. These photoinduced phenomena coupled with the PCO properties of TiO<sub>2</sub> are at the basis of the self-cleaning properties of TiO<sub>2</sub>-covered glasses and walls.

### 3. Preparation of MTTFs

#### 3.1. Synthetic aspects

TiO<sub>2</sub> nanomaterials can be classified according to their shape and dimension: 0D nanomaterials refer to nearly spherical nanoparticles (quantum dots); 1D refers to nanowires, nanobelts, and nanorods; and 2D materials correspond to thin films, while 3D is used to indicate porous nanostructures.

Mesoporous thin films have very peculiar features, particularly high surface area, controlled porosity, high flexibility in composition, and surface design [24]. For practical applications, mesoporous thin films must possess a number of general features: (i) they must be continuous and free of crack; (ii) crystalline walls are highly desirable in order to process into functional materials; and (iii) pores must be accessible, preferably from the film surface [25]. As a matter of fact, unlike powder, the internal space of a mesoporous thin film may not be accessible unless there are pores opening at the surfaces [26].

Mesoporous materials can form various pore structures including hexagonal (*p6mm*), cubic (*Ia3d*, *Im3m*, and *Pm3m*), and disorganized structures (**Figure 3**). Although the hexagonal structure is the most encountered one due to its easy synthetic procedure, this structure has a drawback in terms of pore accessibility when obtained as thin films, since the interfacial energy between the substrate surface and the film materials often lead to the pores laying parallel to the substrate surface [25]. For this reason, recent development of synthesis protocols of mesoporous titania thin films has been achieved to access to cubic structures or to hexagonal structures with aligned vertical pores.

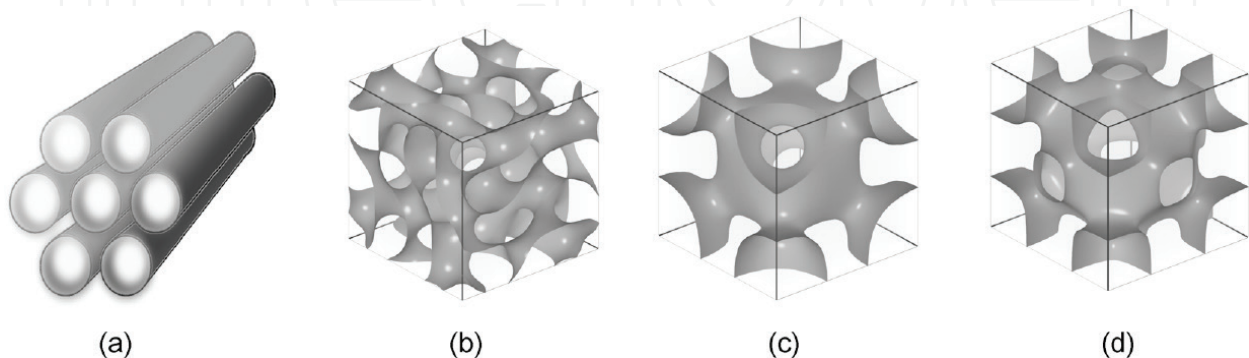


**Figure 3.** A representation of the structures found in mesoporous materials: (a) hexagonal, (b) cubic (*Ia3d*), (c) cubic (*Im3m*), and (d) cubic (*Pm3m*) (from Ref. 25).

The first mesoporous thin films, which have been the object of extensive studies, were essentially silica-based and structure-directing agents, such as surfactants, were used for their synthesis. The formation mechanism of these materials involves the self-assembly of the templates in supramolecular structures, such as micelles, with the inorganic species associated to their hydrophilic portions. Simultaneously, the inorganic precursor undergoes hydrolysis and condensation reactions [25].

In general, the synthesis of mesoporous materials of transition metal oxides is more difficult than that of silica. A reason may be found in the fact that the hydrolysis and condensation reactions of transition metal ions are much faster (often hard to control due to the excessive rate) with respect to silicon-based precursors. Consequently, the inorganic precursor is prevented to effectively associate with the templates during condensation, and often mesoscopic disorder is obtained in the resulting material [27]. This high reactivity of transition metal precursors, compared to silicates, is attributed to the lower electronegativity of the metal and to its ability to exhibit several coordination states, so that the coordination expansion occurs spontaneously upon reaction with water or other nucleophilic reagents [28]. In order to minimize this problem, the precursor solution of Ti is often strongly acidic enough to suppress the hydrolysis and condensation reactions, so that the film material forms a liquid crystal-like state [29].

The synthetic approach adopted for mesoporous titania thin films (MTTFs) is often a combination between the sol-gel chemistry of an inorganic precursor and the self-assembly process of an organic template (evaporation-induced self-assembly (EISA)). The sol-gel process is a synthesis route which involves the preparation of a "sol" and the subsequent gelation upon the solvent removal. A "sol" consists of a liquid with colloidal particles which are not dissolved, but do not agglomerate or sediment. A gel consists of a three-dimensional continuous network, which includes a liquid phase. Sol-gel syntheses can use either a metal-organic precursor or an inorganic precursor. In both cases, a dilute, usually an acidic solution of precursor and an amphiphilic organic template, is introduced in a volatile solvent containing a specific amount of water. The solution is spin- or dip-coated onto virtually any type of substrate. Upon evaporation of the organic solvent, the system self-organizes to form a periodic inorganic-organic composite. As a matter of fact, surfactants can spontaneously self-assemble in micelles when their concentration in a given solvent is higher than the critical micellar concentration (CMC). At higher concentration, micelles can assemble in liquid crystalline arrays. A thermal posttreatment is often used to proceed to the cross-linking of the inorganic framework together with the removal of the organic template, leading, in turn, to the formation of the mesoporous thin film. The two more often encountered pore structures are either a cubic lattice displaying three-dimensionally interconnected pores or channel-like pores arranged in a hexagonal array [30]. Adjustment of the pore architecture of mesoporous materials strongly affects their properties, such as adsorption affinity toward guest molecules and photocatalytic properties of materials [16].

### 3.2. The $\text{TiO}_2$ precursor candidates

Two classes of precursor for the preparation of mesoporous thin films can be used: (i) inorganic precursors and (ii) metal-organic precursors.

Inorganic precursors are salts that produce in water-solvated cations. The charge transfer from the bonding orbitals of water molecules to empty the orbitals of transition metals makes the water molecules more acidic. Different water complexes can form depending on the magnitude of this electron transfer. A condensation may take place via olation in which a hydroxyl bridge is formed between two metal centers. Olation occurs by a nucleophilic substitution ( $S_N$ ) where the hydroxyl group is the nucleophile and water is the leaving group; however, oxolation can also occur in which an oxo bridge is formed between two metal centers. Oxolation proceeds through two consecutive steps: the first step is a nucleophilic addition between hydroxy precursors, and the second step is water elimination [28].

Metal-organic precursors are usually metal alkoxides which are more reactive due to the presence of highly electronegative OR groups that stabilize the metal center in the highest oxidation state and render it more susceptible to nucleophilic attack. Hydrolysis and condensations occur by nucleophilic substitution involving a nucleophilic addition followed by a proton transfer and removal of protonated species (via olation or oxolation mechanisms).

In order to prepare MTTFs, titanium chloride (TiCl<sub>4</sub>), titanium alkoxides (mostly used tetraisopropoxide or tetraethoxide), and tetrabutyl titanate (TBT) are often used as titanium sources. Handling titanium chloride requires careful attention since it reacts violently with water and high humidity atmosphere in fast exothermic hydrolysis reactions. In this case, alcoholysis or hydrolysis processes release protons that acidify the solution, a necessary step to promote polymerization. Titanium alkoxides are highly reactive and highly hygroscopic precursors requiring to be handled within a moisture-free environment. To induce the polymerization of the inorganic framework, in the case of titanium alkoxides, addition of strong acid such as HCl required, or in alternative, the use of specific chelating agents. HCl is, however, the preferred choice for the production of MTTFs since its high volatility does not impede the efficiency of the evaporation-assisted deposition [13].

### 3.3. The templating agents

A variety of templates, such as alkyl phosphate anionic surfactants [31], quaternary ammonium cationic templates [32, 33], primary amines [34, 35], and poly(ethylene oxide)-based surfactants [29, 36], have been used to manipulate the pore structures of titania. Nonetheless, to direct and control the morphology of the inorganic framework for the preparation of mesoporous thin films, block copolymers seem to be the more frequently chosen templating agents since their self-assembly properties are driven by evaporation. However, the choice and combination between the Ti source and the templating agent are the crucial steps for the successful preparation of highly organized mesoporous TiO<sub>2</sub> thin films [37]. Hard- and soft-templating syntheses are the two most widely used methods to prepare these porous materials. A comprehensive description of both routes is given in the excellent book chapter written by Bonelli et al. [38], to which interested readers are referred.

The mostly employed soft-template-assisted route takes advantage of the self-assembly properties of organic ionic surfactants or neutral polymeric surfactants allowing to access to a diversity of supramolecular structures ranging from spherical micelles to hexagonal rods and lamellar liquid crystals. The formation of these supramolecular assemblies is governed by

non-covalent weak interactions in particular hydrogen bonding, van der Waals forces, and electrostatic interactions. These assemblies are in situ used as soft templates allowing the tuning of the pore size and organization within the resulting porous materials. PEO (polyethylene oxide)-based templates have been extensively used in soft-template synthesis of mesoporous thin films. A study by Stucky [36] suggested that non-hydrolytic reactions take place in their low-water-content systems, allowing the oxide network to be built in a more controlled way. The proposed mechanism suggested that, once the metal center is trapped by the PEO or PPO fragments, nucleophilic reactions occur between the cationic immobilized species, leading to the formation of oligomers attached to the polymer chains. These oligomers are anchoring points for the growing inorganic phase [39].

PEO containing block copolymers are often chosen as the preferred templates since they can easily be produced in variable lengths, allowing in turn to generate differently shaped templates. Furthermore, PEO blocks are highly hydrophilic and favorably interact with Ti-oxo hydrophilic species in solution stabilizing upon drying the inorganic/organic interface at the shell of the formed micelles [39]. Indeed, the relative size of the hydrophilic and hydrophobic domains is in great part responsible for the symmetry of the pore array. After mixing with surfactant followed by casting into thin films, this mixture turns into a liquid crystal-like state, which, in due course, self-assembles into mesostructures on aging under controlled temperature and humidity conditions [27].

The choice of the surfactant is also an influence on the type of mesostructure obtained. It was reported that while Brij 58  $-(EO)_{20}-C_{16}H_{33}-$  leads to an  $Im3m$  mesoporous structure, the Brij 56, characterized by a smaller hydrophilic domain, leads to hexagonally packed cylindrical micelles with a  $p6mm$  symmetry [29].

In a recent study, Lee et al. [27] investigated the influence of the surfactant concentration and reported that a concentration equal to 9% wt for Brij 58 led to an  $Im3m$  mesoporous structure. Ozin et al. [40, 41] indicated that mesoporous titania thin film having anatase walls can be prepared using triblock copolymers as template materials. According to these reports, the templating agent is also able to affect the crystallinity of the MTTF. Indeed, Innocenzi et al. [42] investigated the above aspect by a correlative analysis of a MTTF and a dense sol-gel titania film (without the block copolymer), prepared under the same conditions; they found that in mesoporous titania thin film (with surfactant) the crystallization to anatase is favored and occurs at lower temperatures.

### 3.4. Depositions techniques

Two main deposition techniques have been widely used to prepare MTTFs, namely, spin-coating or dip-coating.

Spin-coating is a simple process for a rapid deposition of thin films onto flat substrates. The substrate to be covered is held by some rotatable fixture (often using vacuum to clamp the substrate into place), and the coating solution is spread onto the surface; the action of spinning causes the liquid to spin radially outward by the centrifugal force until the thin film is formed. The initial volume of the fluid distributed onto the rotating substrate and the delivery rate have both a minor effect onto the final film thickness. On the other hand, the resulting viscosity

of the fluid to be deposited and the chosen ultimate rotation velocity are both parameters that mainly control the resulting thickness of the film. High angular speed produces thinner film. At a constant speed, the film thickness initially rapidly decreases, but this decrease slows at longer times. Typical coating thickness values are often below 1  $\mu$  when spin-coating is used.

Dip-coating is a technique based on the deposition of a wet liquid film by withdrawal of a substrate from a liquid coating medium. This process is very simple, flexible, and economically advantageous. Nevertheless, it is necessary to make provisions for cleanliness in order to obtain a high-quality deposition. Dip-coating is one of the few techniques that allow a simultaneous double-sided coating which may be regarded as an advantage especially in production of optical filters. Typically, film thickness obtained with dip-coating ranges from a few nanometers to 200 nm for oxide coatings. The thickness of the liquid film depends mainly on two factors: (i) the viscosity of the solution and (ii) the speed rate used during the substrate withdrawn from the solution.

In dip-coating, mesoscale ordering is achieved almost instantly after the covered substrate is withdrawn from the solution. Even if the self-assembled structure may form by spin-coating, the degree of ordering cannot be as high as in the case of dip-coating. This is probably due to the faster solvent evaporation occurring during spin-coating leading to a more viscous film deposit, which, in turn, makes the rearrangement of the titania and surfactant species in solution that is too sluggish to achieve a high degree of ordering in a short period of time [26].

### 3.5. Aging conditions

Several parameters such as temperature, aging period, and relative humidity have to be taken into account during the aging phase. Indeed, they all have important effects onto the final mesoporous structure in titania-based system. The evaporation process during the aging period after the spin- or dip-coating deposition plays a critical role not only for the formation of ordered porosity but also to direct the symmetry displayed by the pore arrays [21]. During the last decade, many research groups have reported the effects of the aging conditions onto the mesostructure of titania thin films, and they confirmed that high humidity conditions are a requisite to access highly ordered mesostructure in titania thin films [29, 43, 44].

During the aging phase, the titania species and the surfactant molecules are in a liquid crystal-like state, and the mesoscopic ordering is achieved through the rearrangement of these species. The moisture inside the as-synthesized film materials plays a dual role. Kinetically, it is a lubricant to facilitate the rearrangement, and, thermodynamically, it is a structural ingredient to form the mesostructures. According to Lee et al. [27], it is important to keep the moisture of the as-synthesized film at a certain level (70%) until the full ordering is achieved. However, it has been observed that too prolonged treatments at humidity rates higher than 70% can be detrimental to the meso-ordering due to excessive water swelling [45]. Ozin et al. [15] have reported that a high humidity level (*ca.* 60%) during aging favors a cubic structure, while a lower humidity level (40%) favors the hexagonal structure. According to various studies, the aging time should not be longer than 72 h, because films may transform to other unidentified structures of lower order [26, 27].

The aging temperature plays also an important role and is often chosen equal to 18°C, as reported in several studies [25, 27]. However, using ethanolic solutions of  $\text{TiCl}_4$  and F127 as surfactants, the mesostructure could be tuned from cubic to hexagonal by aging at 18°C or 35°C, respectively [27].

In contrast to most studies, Oveisi et al. [16] recently reported that highly ordered mesostructures can be reached when the condensation reaction of metal alkoxides is occurring after the formation of the liquid crystal thin-film covering (after complete evaporation of solvents). This hypothesis was confirmed by working under non-usual aging conditions: lower temperature (−20°C) and lower humidity (20% RH).

### 3.6. Thermal posttreatment

After the aging phase, titania thin films are calcinated at high temperature. In this step, a sequence of transformations takes place: evaporation of the remaining solvent and acid ( $T < 200^\circ\text{C}$ ) which activates consolidation of the framework (this step is accompanied by an uniaxial shrinkage of the mesostructure along the  $z$  axis); template pyrolysis ( $T = 250\text{--}300^\circ\text{C}$ ), which generates the porosity; and crystallite nucleation and growth on walls ( $T > 300^\circ\text{C}$ ) [9].

Typically with mesoporous  $\text{TiO}_2$ , the thermal posttreatment effectuated to convert the amorphous titania walls into crystalline walls usually results in the partial or total collapse of the mesoporous network [46, 47]. To circumvent such a drawback, several post-synthesis treatments have been developed mainly devoted to increase the thermal stability of the mesoporous  $\text{TiO}_2$ . In particular, Cassiers et al. [48] reported that the posttreatment of an uncalcinated mesoporous titania powder with ammonia resulted in the formation of mesoporous crystalline titania with thermal stability up to 600°C. Sanchez and coworkers [49] claimed that the mesoporous anatase network could be retained with a porosity of 35% above 650°C by applying a specific post-synthesis delayed rapid crystallization (DRC) treatment. Another study demonstrates that the thermal stability of these crystalline films can be enhanced, up to 850°C, by posttreatment of the film in supercritical carbon dioxide ( $\text{sc-CO}_2$ ) with the presence of a small amount of precursor, such as tetramethoxysilane (TMOS) [50].

The thermal posttreatment has to be therefore carefully done and monitored especially if a specific  $\text{TiO}_2$  polymorph is sought. Most of the reported literature data available are dedicated to the preferential formation of anatase vs. the rutile polymorph. Although through the literature a large inhomogeneity in temperature range over the control of a selected polymorph is present and reflects the influence of secondary important factors such as the Ti precursor, the template, the deposition technique, and the experiment conditions used to form the  $\text{TiO}_2$  mesoporous material [51], most of the reports agree in the temperature range of 350–450°C to promote the exclusive crystallization of the anatase polymorph, while at higher temperature, the rutile phase transformation initiate [42, 52].

### 3.7. Alignment of the pores

As previously mentioned, the pores of the thin films must be accessible. Indeed, many potential applications of mesoporous thin films are relying on the accessibility of the pores from

the surface. Owing to interfacial orientation preferences between the substrate and the material, the 2D hexagonal mesoporous thin films present their pore channels parallel to the surface [25]. For this reason, many research groups have struggled to synthesize cubic mesoporous thin films, which present, regardless of the orientation, pore openings from their surfaces owing to their intrinsic geometry [44, 49–53]. Often, the solution resides in the optimization of the composition of the precursor solution performed by varying the ratios between quantity of surfactant and inorganic precursor [25, 54, 55]. In this context, Koganti et al. [56] showed that a modification of the substrate surface with a Pluronic block copolymer could lower the surface energy and induce the channels to tilt away from the substrate plane. Other groups have varied the aging temperature to form cubic structures [57]. Lee et al. [26] reported the preparation of MTTFs with vertical pores using TiCl<sub>4</sub> as source of titanium, F127 as surfactant, and by applying a specific heat treatment to direct the formation of the 3D network in a cubic phase. Zhou et al. [7] formed MTTFs with vertical pores, by calcination of the film at 450°C, so that the 3D hexagonal mesostructure was transformed to a grid-like mesostructure with quasi-perpendicular porosity through sintering-diffusion and pore merging along the c-axis. Richman et al. [30] used another approach: they synthesized mesoporous films through nanometer-scale epitaxy. They prepared a titania thin film with cubic symmetry and used it as a patterned substrate to direct a hexagonal top silica mesostructured with vertically oriented pore channels. Finally, Yamauchi et al. applied a very strong magnetic field (10T) in mesoporous silica films to align the channels, but the alignment was not homogeneously perfect, and such method remains rather impractical for large areas [58].

#### 4. MTTF characterizations

Beyond the synthesis of MTTFs, it is necessary to deeply characterize their structure, in particular the type of pore arrays, the film thicknesses, the porosity (pore volume, pore size distribution, interconnectivity, and specific surface area), the surface topography, the chemical composition, and the crystallinity grade. The most commonly used characterization techniques for MTTFs are microscopies such as SEM, TEM, or AFM; spectroscopic techniques such as UV-Visible spectroscopy or ellipsometry (E), Fourier transform infrared spectroscopy (FTIR), and Raman spectroscopy; X-ray absorption techniques like XANES and EXAFS; and powder or small-angle X-ray diffraction (XRD).

Spectroscopic ellipsometry (E) is an optical measurement technique based on the change in polarization occurring at many wavelengths. Ellipsometry is often highly sensitive to the properties of 1 nm to 10 μ thick films. The spectral response provides information about the sample properties, such as film thickness, surface conditions such as surface roughness (or the presence of surface contaminants), film thickness uniformity, anisotropy, and some important physical properties, such as refractive index [59]. Fourier transform infrared spectroscopy (FTIR) is a fast, contactless, and nondestructive technique used to control the complete removal of the template and the presence of organic groups. Raman spectroscopy is a useful technique used to determine titania crystalline phase by analyzing the Ti-O-Ti vibrations in the 200–600 cm<sup>-1</sup> region. XANES and EXAFS had been used to accurately probe and characterize the Ti(IV) environment in solution and within the final material.

Electron microscopies SEM and TEM are local techniques and should be used as complementary techniques to diffraction. Scanning electron microscopy (SEM) is perhaps the most widely employed thin film and coating characterization instrument. It shows the surface pore arrangement giving information on the MTTF surface morphology. Atomic force microscopy (AFM) provides imaging topography of the sample surface, so it is a local but a very useful technique. The use of a very sharp probe that is scanned across the thin-film surface allows to produce very high-resolution topographic images at the sub-nanometer scale. Many different imaging modes are available in AFM, such as contact mode imaging which works in the repulsive regime because the probe remains in contact with the sample at all times, noncontact mode which works in the attractive regime because the probe is very close to the sample surface without touching it, and tapping mode which works in both the regimes. Tapping mode AFM is the most used mode in the case of titania thin films, whereby a sharp tip (typically, a silicon or silicon nitride crystal) is oscillated above the surface of a sample. Specifically, tapping mode overcomes major problems associated with friction, adhesion, electrostatic forces, and other tip-sample-related issues (**Figure 4**).

X-ray diffraction in Bragg-Brentano geometry is a noncontact and nondestructive technique that provides information about crystallinity, phase, crystallite size, and orientation. Comparison of the obtained XRD profile in the medium and wide-angle region (from  $2\theta = 10$  to  $80^\circ$ ) with reference patterns allows to determine the crystalline phase of the MTTFs as well as possible preferential orientational order through the increase in intensity of specific reflection peaks. The XRD patterns of the three main crystalline phases of  $\text{TiO}_2$  are reported in **Figure 5**.

The analysis of XRD patterns must be carefully performed to correctly identify the crystalline phase of the MTTFs, especially when polymorphic forms are present within the film. This task is also often complicated by the presence of the wide halo of the amorphous substrate onto which the MTTF films have been deposited and/or the superposition of the reflection peaks relative to the eventual semicrystalline nature of the substrate used (e.g., when the  $\text{TiO}_2$  thin film is deposited on ITO). In **Figure 6** an XRD pattern of a dense anatase  $\text{TiO}_2$  thin film deposited on a glass substrate is reported [60], clearly showing the broadening of the background level due to the halo generated by the amorphous support.

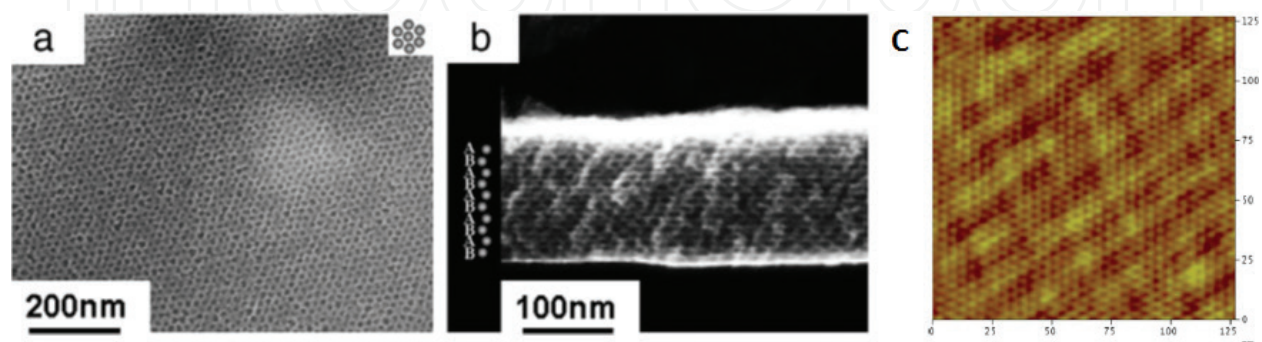


**Figure 4.** (a) Top surface and (b) cross-sectional FESEM micrographs of the 3D hexagonal MTTF [7] and (c) AFM image of MTTF surface [27].

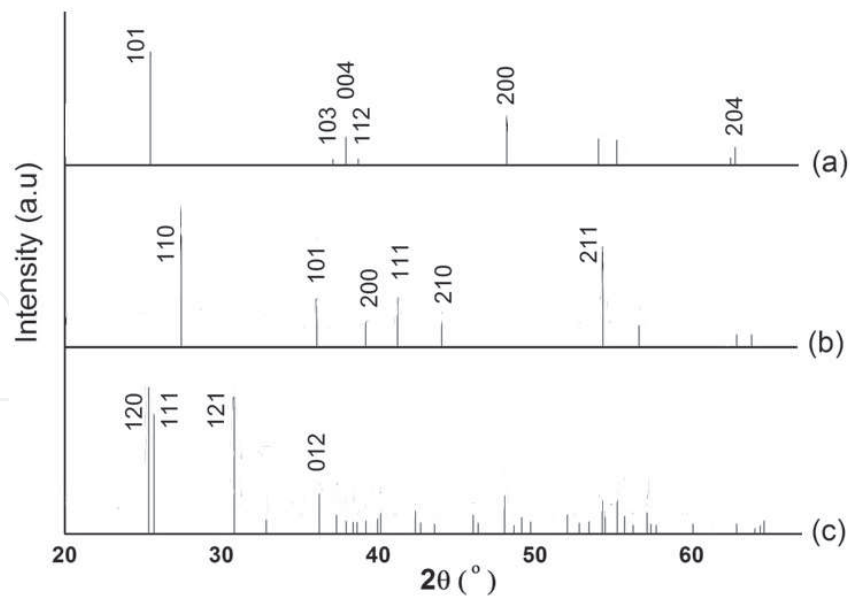


**Figure 5.** XRD patterns of (a) TiO<sub>2</sub> anatase (JCPDS card no. 21-1272), (b) TiO<sub>2</sub> rutile (JCPDS card no. 21-1276), and (c) TiO<sub>2</sub> brookite (JCPDS card no. 29-1360).

While there are no difficulties in discriminating between the anatase and the rutile phases since the first two reflection peaks are well separated ( $2\theta = 25.28^\circ$  for  $d_{101}$  of anatase vs.  $2\theta = 27.44^\circ$  for  $d_{110}$  of rutile), spotting the difference between anatase and brookite might be more tricky. Only, the reflection peaks at  $2\theta = 30.81^\circ$  relative to the  $d_{121}$  of the brookite phase or at  $2\theta = 62.57^\circ$  relative to  $d_{204}$  of the anatase phase can help in making such a difference and/or recognize the presence of both the polymorphic forms in an XRD pattern [61].

A small-angle diffraction pattern, instead, could reveal the eventual presence of an ordered array of mesopores within the MTTFs, allowing the determination of its geometry, i.e., cubic lamellar or hexagonal [44, 62], as shown in **Figure 7**.

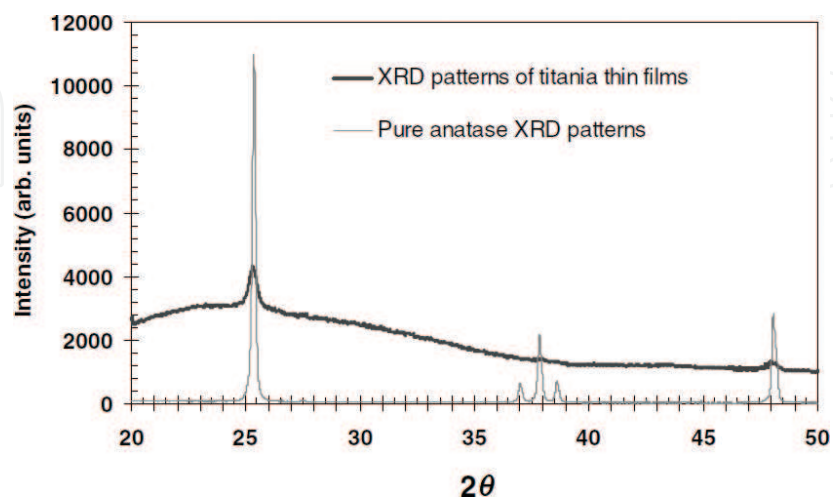


**Figure 6.** XRD patterns of a dense TiO<sub>2</sub> thin film prepared by sol-gel and dip-coating techniques on a glass substrate (from Ref. 60).

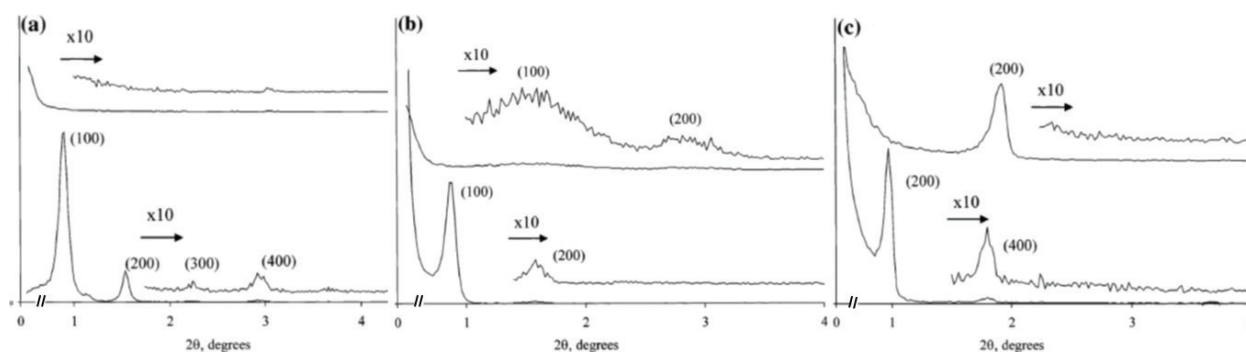


**Figure 7.** Small-angle XRD patterns of  $\text{TiO}_2$  thin films, as-synthesized (bottom) and calcined (top) films for (a) lamellar, (b) hexagonal, and (c) cubic titania mesostructures (figures adapted from Ref. 62).

#### 4.1. Evaluation of the photocatalyst activity

The activity of a photocatalytic titania mesoporous thin film can vary considerably depending on many factors, such as crystallinity, surface-to-volume ratio, pore accessibility, film thickness, and roughness. The photocatalytic activity of MTTFs can be determined evaluating the decomposition of stearic acid (SA), used as probe, under UV illumination ( $\lambda = 256 \text{ nm}$ ). This fatty acid is usually chosen for its high stability under UV illumination in the absence of suitable photocatalyst film. Furthermore, a thin layer of stearic acid can easily be deposited through dip- or spin-coating onto the film from a methanol or chloroform solution. SA provides a reasonably good model compound for solid films since it undergoes oxidative mineralization and this process can be monitored as a function of time [63]:

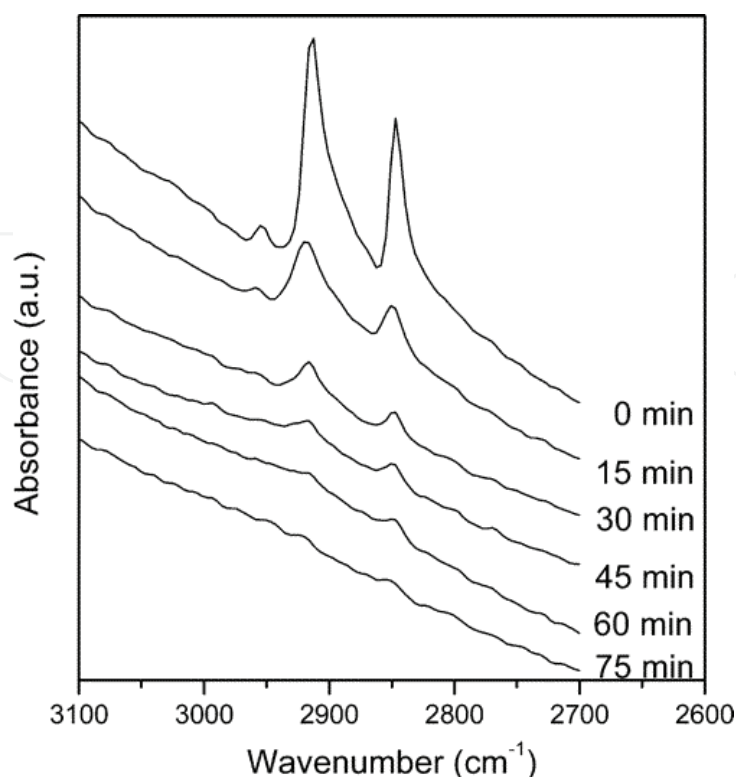
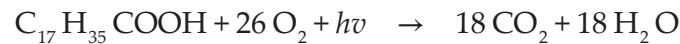


**Figure 8.** Disappearance of the stearic acid IR bands (C–H stretches at  $2912$  and  $2847 \text{ cm}^{-1}$ ) on the surface of a titania thin film after irradiation with UV light ( $\lambda = 256 \text{ nm}$ ) [64].



SA decomposition can be demonstrated, for example, by FTIR spectroscopy through the monitoring of the asymmetric C-H stretching mode of the CH<sub>3</sub> group at 2958 cm<sup>-1</sup> and the asymmetric and symmetric C-H stretching modes of the CH<sub>2</sub> group at 2923 and 2853 cm<sup>-1</sup>, respectively (**Figure 8**) [64].

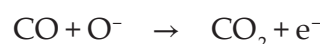
The photocatalyst activity of titania can also be evaluated via photocatalytic oxidation of methylene blue (MB) under UV illumination. MB is often used as model for recalcitrant azo-dye pollutant, and, being a highly colored organic molecule, its photodecomposition can easily be detected in situ through spectrophotometric methods [65].

## 5. Applications of MTTFs

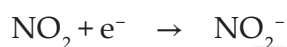
Mesoporous TiO<sub>2</sub> thin films have attracted researchers among various fields of applications spanning from sensors, self-cleaning coatings, lithium-ion batteries (LIBs), photocatalysis, and new-generation solar cells. For interested readers, three comprehensive reviews, on the photocatalytic applications of mesoporous TiO<sub>2</sub>-based materials [38], on the use of TiO<sub>2</sub>-ordered materials for solar radiation applications [66], and on the self-cleaning applications of TiO<sub>2</sub> [67], have recently been published. The present section will therefore only cover the applications of mesoporous TiO<sub>2</sub> in sensor and LIB applications.

### 5.1. Sensors

A good sensor requires high sensitivity, fast response, and good selectivity. Furthermore, low-cost materials and easy fabrication processes are important advantages for practical uses. Mesoporous titania thin films are excellent candidates for sensing applications because of the enhancement of the sensing signal due to the increased surface. Nevertheless, the MTTF sensitivity is also affected by the pore size and the carrier's diffusion length. The sensing mechanism includes three steps: initially, TiO<sub>2</sub> surface binds the analyte molecules; subsequently, a specific chemical or biochemical reaction takes place at the interface and gives rise to a chemical signal, converted, in the third step, into an electronic signal in turn amplified and detected. TiO<sub>2</sub> sensors can detect several gases, including either oxidative gas (O<sub>2</sub>, NO<sub>2</sub>) or reductive gas (H<sub>2</sub>, CO, NH<sub>3</sub>). The working principle of these sensors relies on the changes of the electronic resistance, due to the interaction of TiO<sub>2</sub> with the surrounding environment. The vacancies on TiO<sub>2</sub> surface play an important role, since oxygen is adsorbed on these surface vacancies when the film is exposed to air forming anionic oxygen. When a gas molecule is in contact with a gas sensor based on MTTFs, first this molecule is physisorbed on TiO<sub>2</sub> surface through van der Waals forces and dipole interactions; immediately after, the gas molecule is chemisorbed via a strong chemical bond formed between the gas and the surface atoms of TiO<sub>2</sub>. In this step, a charge transfer induced by the redox reaction between titania and the gas molecule occurs [68]. When a reducing gas (e.g., CO) is detected by a chemical sensor, the following reaction takes place:



In this case, CO molecules react with adsorbed oxygen ions on the mesoporous film surface, which results, in turn, in an overall decrease of the electrical resistance of the metal oxide thin films. On the contrary, if a chemical sensor is exposed to an oxidation gas (e.g., NO<sub>2</sub>), the following oxidizing reaction may take place:



In this example, NO<sub>2</sub> molecules cause a depletion of electrons from the TiO<sub>2</sub> surface, which results in an increase of electrical resistance. The conductivity change can be easily transferred into resistance signal, which is the best-known sensor output signal.

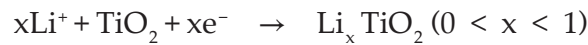
Titania nanostructured materials are good candidates also for biosensing, because TiO<sub>2</sub> is able to form coordination bonds with the amine and the carboxylic groups of biomolecules, such as enzymes, while maintaining the enzyme's biocatalytic activity. Furthermore, TiO<sub>2</sub> is characterized by high stability and biocompatibility. A biosensor is an analytical device, which converts a biological response into readable or quantified signal. Biosensors can be applied to analyze a variety of samples including body fluids, food samples, and cell cultures [68]. The biosensing mechanism is based on a biochemical reaction. Typically in (bio-)electrochemistry, a measurable current (amperometric), a measurable potential, or a charge accumulation (potentiometric) will be generated upon the alteration of the conductive properties of a medium between electrodes when the sensing takes place.

Titania mesoporous thin films have been also used as sensors for *Escherichia coli*, an enterohemorrhagic bacterium whose infections have a low incidence rate but can have severe and sometimes fatal health consequences and thus represent some of the most serious diseases due to the contamination of water and food [69]. Titania films treated with APTES ((3-aminopropyl) triethoxysilane) and GA (glutaraldehyde) were functionalized with specific antibodies anti-*Escherichia coli* antibodies. In this case, FTIR spectroscopy has been used as an optical transduction method: the spectroscopic signals originated from the various functional groups related to proteins, lipid, and carbohydrates can be used for the identification and structural characterization of different pathogens and subspecies.

## 5.2. Lithium-ion batteries (LIBs)

Lithium-ion batteries (LIBs) are rechargeable batteries widely used in laptop, mobile phones, and electric vehicles. These batteries are characterized by high-energy density, low maintenance, little self-discharge, and no memory effect, which means that it is not necessary to completely discharge them before charging. In a conventional LIB cell, lithium metal oxide (e.g., LiCoO<sub>2</sub>) is used as cathode, while graphite is used as preferred anode. The two electrodes are separated by a porous membrane and soaked in a nonaqueous liquid electrolyte. During insertion (or intercalation), ions move into the electrode. During the reverse process, extraction (or de-intercalation), ions move back out. Upon charging, the lithium ions move from the cathode to enter the anode, while in the discharging phase, the reverse phenomenon takes place. A variety of metal oxides, in particular TiO<sub>2</sub>, have been investigated as potential electrode materials for LIBs. Compared with the currently commercialized graphite anode, these metal oxide materials have demonstrated various advantages, such as very high capacity,

widespread availability, good stability, and environmental benignity. Generally, the reversible reaction between Li and TiO<sub>2</sub> can be expressed by the following equation:



where  $x$  is the mole fraction of Li in TiO<sub>2</sub>. This redox reaction typically takes place at around 1.7 V vs. Li<sup>+</sup>/Li. Lithium ions reversibly insert/extract into/from the interstitial vacancies of the TiO<sub>2</sub> framework, with a specific percentage depending on the TiO<sub>2</sub> crystalline form and morphology. Specifically, anatase is probably the most electrochemically active form of TiO<sub>2</sub> for this purpose [8]. Moreover, it has been demonstrated that anatase exposing (001) facets exhibits efficient Li<sup>+</sup> ion diffusion along this direction (c-axis) facilitating a fast lithium insertion/extraction [70].

TiO<sub>2</sub> presents many advantages in its usage as anode material for LIBS, such as the low-volume expansion upon lithiation (<4%), good stability, and lack of lithium plating. However, TiO<sub>2</sub> is also characterized by some limitations, including a limited Li<sup>+</sup> ion diffusion, low capacity, and low electrical conductivity [71]. A possibility to overcome these drawbacks is represented by the nanostructuring of TiO<sub>2</sub>, which provides a higher specific surface area and shorter diffusion pathways for electrons and Li<sup>+</sup> ions, compared to the corresponding bulk materials [72]. In this context, vertically oriented TiO<sub>2</sub> nanotubes have been exploited as anode materials for LIBs by many groups [73–75]. However, the preparation of nanostructured TiO<sub>2</sub> in the form of mesoporous thin films could offer some advantages, such as higher specific surface area and thinner walls than a TiO<sub>2</sub> nanotube array [76]. For example, Ortiz et al. prepared mesoporous titania thin films on titanium substrates, with a hexagonally ordered porous structure, and they tested these samples as anode materials for LIBs, reporting an improved electrochemical performance, without the necessity of additives to enhance the transport properties of the electrode [77]. The enhanced electrochemical activity was ascribed to the higher area and volumetric capacity of these films due to the presence of the 3D-ordered mesostructure.

## 6. Conclusions and perspectives

Undeniable great progresses have been made in recent years in the design and synthesis of mesoporous TiO<sub>2</sub> thin films featuring novel and well-designed structures and morphologies as well as to further explore and enhance their applications. Nevertheless, challenges are remaining in developing cheap, low toxic, and reproducible synthetic approaches for achieving an easy and precise control over the pore size, wall thickness, surface area, morphology, and crystallinity.

For optoelectronic applications, the main concern resides into the deposition of organized MTTFs onto semiconductive electrodes such as ITO or FTO keeping a homogenous disposition of the pores on the whole device electrode, and although some preliminary attempts have been made [52, 78], it remains a challenging issue owned to the wettability difference between ITO and Si wafers. Moreover, while small-sized devices have been tested, on large scale, difficulties are encountered to maintain such uniform orientation of the pores, especially in

the case of vertically aligned pore arrays, the most suited geometry for efficient optoelectronic devices. For these reasons, scientists are investigating also the possibility of depositing nanotubes of TiO<sub>2</sub> from anodization of sputtered titanium onto different substrates. The best results have been so far obtained for depositions performed onto quartz. However, in the case of semiconductive substrates, several problems are arising, the most important one being the easy loss of contact between the formed TiO<sub>2</sub> nanotubes and the semiconductive layer, which will definitely require further and intense research activities to circumvent such a drawback.

## Author details

Francesca Scarpelli<sup>1</sup>, Teresa F. Mastropietro<sup>2</sup>, Teresa Poerio<sup>2</sup> and Nicolas Godbert<sup>1\*</sup>

\*Address all correspondence to: nicolas.godbert@unical.it

1 MAT-INLAB Laboratory, Department of Chemistry and Chemical Technologies, University of Calabria, Arcavacata di Rende, CS, Italy

2 Institute on Membrane Technology (ITM-CNR), The University of Calabria, Rende, CS, Italy

## References

- [1] Liu P, Lee SH, Tracy CW, Yan Y, Turner JA. Preparation and lithium insertion properties of mesoporous vanadium oxide. *Advanced Materials*. 2002;**14**(1):27-30. DOI: 10.1002/1521-4095(20020104)14:1<27::AID-ADMA27>3.0.CO;2-6
- [2] Mamak M, Coombs N, Ozin G. Mesoporous yttria-zirconia and metal-yttria-zirconia solid solutions for fuel cells. *Advanced Materials*. 2000;**12**(3):198-202. DOI: 10.1002/(SICI)1521-4095(200002)12:3<198::AID-ADMA198>3.0.CO;2-2
- [3] Mamak M, Coombs N, Ozin G. Self-assembling solid oxide fuel cell materials: Mesoporous yttria-zirconia and metal-yttria-zirconia solid solutions. *Journal of the American Chemical Society*. 2000;**122**(37):8932-8939. DOI: 10.1021/ja0013677
- [4] Frindell KL, Bartl MH, Popitsch A, Stucky GD. Sensitized luminescence of trivalent europium by three-dimensionally arranged anatase nanocrystals in mesostructured titania thin films. *Angewandte Chemie International Edition*. 2002;**41**(6):959-962. DOI: 10.1002/1521-3773(20020315)41:6<959::AID-ANIE959>3.0.CO;2-M
- [5] Grätzel M. Mesoporous oxide junctions and nanostructured solar cells. *Current Opinion in Colloid & Interface Science*. 1999;**4**:314-321. DOI: org/10.1016/S1359-0294(99)90013-4
- [6] Takahara Y, Kondo JN, Takata T, Lu D, Domen K. Mesoporous tantalum oxide. 1. Characterization and photocatalytic activity for the overall water decomposition. *Chemistry of Materials*. 2001;**13**(4):1194-1199. DOI: 10.1021/cm000572i

- [7] Zhou H, Wang C, Feng Z, Li S, Xu B. Formation of grid-like mesoporous titania film via structural transformation and its surface superhydrophilicity conversion. *Surface & Coatings Technology*. 2012;**207**:34-41. DOI: org/10.1016/j.surfcoat.2012.04.067
- [8] Wu HB, Chen JS, Hing HH, Lou XW. Nanostructured metal oxide-based materials as advanced anodes for lithium-ion batteries. *Nanoscale*. 2012;**4**:2526-2542. DOI: 10.1039/C2NR11966H
- [9] Ochiai T, Fujishima A. Photoelectrochemical properties of TiO<sub>2</sub> photocatalyst and its applications for environmental purification. *Journal of Photochemistry and Photobiology C: Photochemistry Reviews*. 2012;**13**(4):247-262. DOI: org/10.1016/j.jphotochemrev.2012.07.001
- [10] Grätzel M. Recent advances in sensitized mesoscopic solar cells. *Accounts in Chemical Research*. 2009;**42**(11):1788-1798. DOI: 10.1021/ar900141y
- [11] Choi H, Stathatos E, Dionysiou DD. Photocatalytic TiO<sub>2</sub> films and membranes for the development of efficient wastewater treatment and reuse systems. *Desalination*. 2007;**202**(1-3):199-206. DOI: org/10.1016/j.desal.2005.12.055
- [12] Zhang L, Bai H, Liu L, Sun DD. Dimension induced intrinsic physio-electrical effects of nanostructured TiO<sub>2</sub> on its antibacterial properties. *Chemical Engineering Journal*. 2018;**334**:1309-1315. DOI: org/10.1016/j.cej.2017.11.075
- [13] Soler-Illia GJAA, Angelomé PC, Fuertes MC, Grosso D, Boissière C. Critical aspects in the production of periodically ordered mesoporous titania thin films. *Nanoscale*. 2012;**4**:2549-2566. DOI: 10.1039/C2NR11817C
- [14] Aksay IA, Trau M, Manne S, Honma I, Yao N, Zhou L, Fenter P, Eisenberger PM, Gruner SM. Biomimetic pathways for assembling inorganic thin films. *Science*. 1996;**273**(5277):892-898. DOI: 10.1126/science.273.5277.892
- [15] Yang H, Kuperman A, Coombs N, Mamiche-Afara S, Ozin GA. Synthesis of oriented films of mesoporous silica on mica. *Nature*. 1996;**379**:703-705. DOI: 10.1038/379703a0
- [16] Oveisi H, Suzuki N, Nemoto Y, Srinivasu P, Beitollahi A, Yamauchi Y. Critical effect of aging condition on mesostructural ordering in mesoporous titania thin film. *Thin Solid Films*, 2010,**518**(23),6714-6719. DOI: org/10.1016/j.tsf.2010.05.112
- [17] Moellmann J, Ehrlich S, Tonner R, Grimme S. A DFT-D study of structural and energetic properties of TiO<sub>2</sub> modifications. *Journal of Physics Condensed Matter*. 2012;**24**(42)-424206). DOI: 10.1088/0953-8984/24/42/424206
- [18] Li J-G, Ishiaki T, Sun X. Anatase, brookite, and rutile nanocrystals via redox reactions under mild hydrothermal conditions: Phase-selective synthesis and physicochemical properties. *Journal of Physical Chemistry C*. 2007;**111**(13):4969-4976. DOI: 10.1021/jp0673258
- [19] Cromer DT, Herrington K. The structures of anatase and rutile. *Journal of the American Chemical Society*. 1955;**77**(18):4708-4709. DOI: 10.1021/ja01623a004
- [20] Baur WH. Atomabstände und bindungswinkel im Brookit, TiO<sub>2</sub>. *Acta Crystallographica*. 1961;**14**:214. DOI: 10.1107/S0365110X61000747

- [21] Turchi CS, Ollis DF. Photocatalytic degradation of organic water contaminants: Mechanisms involving hydroxyl radical attack. *Journal of Catalysis*. 1990;**122**(1):178-192. DOI: [org/10.1016/0021-9517\(90\)90269-P](https://doi.org/10.1016/0021-9517(90)90269-P)
- [22] Sze Tung W, Daoud WA. Self-cleaning fibers via nanotechnology: A virtual reality. *Journal of Materials Chemistry*. 2011;**21**:7858-7869. DOI: [10.1039/C0JM03856C](https://doi.org/10.1039/C0JM03856C)
- [23] Fujishima A, Rao TN, Tryk DA. Titanium dioxide photocatalysis. *Journal of photochemistry and photobiology C: Photochemistry Reviews*. 2000;**1**(1):1-21. DOI: [org/10.1016/S1389-5567\(00\)00002-2](https://doi.org/10.1016/S1389-5567(00)00002-2)
- [24] Innocenzi P, Malfatti L. Mesoporous thin films: Properties and applications. *Chemical Society Reviews*. 2013;**42**:4198-4216. DOI: [10.1039/C3CS35377J](https://doi.org/10.1039/C3CS35377J)
- [25] Lee UH, Kim MH, Kwon YU. Mesoporous thin films with accessible pores from surfaces. *Bulletin of the Korean Chemical Society*. 2006;**27**(6):808-816. DOI: [org/10.5012/bkcs.2006.27.6.808](https://doi.org/10.5012/bkcs.2006.27.6.808)
- [26] Koh CW, Lee UH, Song JK, Lee HR, Kim MH, Suh M, Kwon YU. Mesoporous titania thin film with highly ordered and fully accessible vertical pores and crystalline walls. *Chemistry: An Asian Journal*. 2008;**3**:862-867. DOI: [10.1002/asia.200700331](https://doi.org/10.1002/asia.200700331)
- [27] Lee HU, Lee H, Wen S, Mho S, Kwon YU. Mesoporous titania thin films with pseudocubic structure: Synthetic studies and applications to nanomembranes and nanotemplates. *Microporous and mesoporous materials*. 2006;**88**(1-3):48-55. DOI: [org/10.1016/j.micromeso.2005.08.017](https://doi.org/10.1016/j.micromeso.2005.08.017)
- [28] Brinker CJ, Scherer GW. *Sol-Gel Science. The Physics and Chemistry of Sol-Gel Processing*. Academic Press INC; 1990. p. 908. ISBN-13: 978-0-12-134970-7. ISBN-10: 0-12-34970-5
- [29] Crepaldi EL, Soler-Illia G, Grosso D, Cagnol F, Ribot F, Sanchez C. Controlled formation of highly organized mesoporous titania thin films: From mesostructured hybrids to mesoporous nanoanatase TiO<sub>2</sub>. *Journal of the American Chemical Society*. 2003;**125**(32):9770-9986. DOI: [10.1021/ja030070g](https://doi.org/10.1021/ja030070g)
- [30] Richman EK, Brezesinski T, Tolbert SH. Vertically oriented hexagonal mesoporous films formed through nanometre-scale epitaxy. *Nature Materials*. 2008;**7**:712-717. DOI: [10.1038/nmat2257](https://doi.org/10.1038/nmat2257)
- [31] Antonelli DM, Ying JY. Synthesis of hexagonally packed mesoporous TiO<sub>2</sub> by a modified sol-gel method. *Angewandte Chemie International Edition in English*. 1995;**34**(18):2014-2017. DOI: [10.1002/anie.199520141](https://doi.org/10.1002/anie.199520141)
- [32] Stone VF, Davis RJ. Synthesis, characterization, and photocatalytic activity of titania and niobia mesoporous molecular sieves. *Chemistry of Materials*. 1998;**10**(5):1468-1474. DOI: [10.1021/cm980050r](https://doi.org/10.1021/cm980050r)
- [33] Yuan Z-Y, Vantomme A, Leonard A, Su B-L. Surfactant-assisted synthesis of unprecedented hierarchical meso-macrostructured zirconia. *Chemical Communications*. 2003;**0**:1558-1559. DOI: [10.1039/B303272H](https://doi.org/10.1039/B303272H)

- [34] Suh Y, Lee J, Rhee H. Synthesis of thermally stable tetragonal Zirconia with large surface area and its catalytic activity in the skeletal isomerization of 1-butene. *Catalysis Letters*. 2003;**90**(1-2):103-109. DOI: org/10.1023/A:1025884714465
- [35] Tian ZR, Tong W, Wang J, Duan N, Krishnan VV, Suib SL. Manganese oxide mesoporous structures: Mixed-valent semiconducting catalysts. *Science*. 1997;**276**(5314):926-930. DOI: 10.1126/science.276.5314.926
- [36] Yang P, Zhao D, Margolese DL, Chmelka BF, Stucky GD. Generalized syntheses of large-pore mesoporous metal oxides with semicrystalline frameworks. *Nature*. 1998;**396**:152-155. DOI: 10.1038/24132
- [37] Wang J, Wu J, Li H. A review of mesoporous TiO<sub>2</sub> thin films. *Material Matters*. 2012;**7**(2):2-6
- [38] Bonelli B, Esposito S, Freyria FS. In: Janus M, editor. *Mesoporous Titania: Synthesis, Properties and Comparison with Non-Porous Titania, Titanium Dioxide*. InTech; 2017. DOI: 10.5772/intechopen.68884
- [39] Soler-Illia GJAA, Sanchez C. Interactions between poly(ethylene oxide)-based surfactants and transition metal alkoxides: Their role in the templated construction of mesostructured hybrid organic-inorganic composites. *New Journal of Chemistry*. 2000;**24**:493-499. DOI: 10.1039/B002518F
- [40] Choi SY, Mamak M, Coombs N, Chopra N, Ozin GA. Thermally stable two-dimensional hexagonal mesoporous nanocrystalline anatase, meso-nc-TiO<sub>2</sub>: Bulk and crack-free thin film morphologies. *Advanced Functional Materials*. 2004;**14**(4):335-344. DOI: 10.1002/adfm.200305039
- [41] Choi SY, Mamak M, Speakman S, Chopra N, Ozin GA. Evolution of nanocrystallinity in periodic mesoporous anatase thin films. *Small*. 2005;**1**(2):226-232. DOI: 10.1002/smll.200400038
- [42] Innocenzi P, Malfatti L, Kidchob T, Enzo S, Della Ventura G, Schade U, Marcelli A. Correlative analysis of the crystallization of sol-gel dense and mesoporous anatase titania films. *Journal of Physical Chemistry C*. 2010;**114**(51):22385-22391. DOI: 10.1021/jp1042766
- [43] Soler-Illia GJAA, Innocenzi P. Mesoporous hybrid thin films: The physics and chemistry beneath. *Chemistry: A European Journal*. 2006;**12**(17):4478-4494. DOI: 10.1002/chem.200500801
- [44] Pan JH, Lee WI. Selective control of cubic and hexagonal mesophases for titania and silica thin films with spin-coating. *New Journal of Chemistry*. 2005;**29**:841-846. DOI: 10.1039/B417310D
- [45] Henderson MJ, Gibaud A, Bardeau JF, White JW. An X-ray reflectivity study of evaporation-induced self-assembled titania-based films. *Journal of Materials Chemistry*. 2006;**16**:2478-2484. DOI: 10.1039/B601677D
- [46] Sayari A, Liu P. Non-silica periodic mesostructured materials: Recent progress. *Micro-porous Materials*. 1997;**12**:149-177. DOI: org/10.1016/S0927-6513(97)00059-X

- [47] Schüth F. Non-siliceous mesostructured and mesoporous materials. *Chemistry of Materials*. 2001;**13**(10):3184-3195. DOI: 10.1021/cm011030j
- [48] Cassiers K, Linssen T, Meynen V, Van Der Voort P, Cool P, Vansant EF. A new strategy towards ultra stable mesoporous titania with nanosized anatase walls. *Chemical Communications*. 2003:1178-1179. DOI: 10.1039/B302116E
- [49] Grosso D, Soler-Illia GJAA, Crepaldi EL, Cagnol F, Sinturel C, Bourgeois A, Brunet-Bruneau A, Amenitsch H, Albouy PA, Sanchez C. Highly porous TiO<sub>2</sub> anatase optical thin films with cubic mesostructure stabilized at 700°C. *Chemistry of Materials*. 2003;**15**(24):4562-4570. DOI: 10.1021/cm031060h
- [50] Wang K, Morris MA, Holmes JD. Preparation of mesoporous titania thin films with remarkably high thermal stability. *Chemistry of Materials*. 2005;**17**(6):1269-1271. DOI: 10.1021/cm047912a
- [51] Girish Kumar S, Koteswara Rao KSR. Polymorphic phase transition among the titania crystal structures using a solution-based approach: from precursor chemistry to nucleation process. *Nanoscale*. 2014;**6**:11574-11632. DOI: 10.1039/C4NR01657B
- [52] Uchida H, Patel MN, May A, Gupta G, Stevenson KJ, Johnston KP. Highly-ordered mesoporous titania thin films prepared via surfactant assembly on conductive indium-tin-oxide/glass substrate and its optical properties. *Thin Solid films*. 2010;**518**(12):3169-3176. DOI: org/10.1016/j.tsf.2009.08.050
- [53] Wang XC, Yu JC, Yip HY, Wu L, Wong PK, Lai SY. A mesoporous Pt/TiO<sub>2</sub> nanoarchitecture with catalytic and photocatalytic functions. *Chemistry: A European Journal*. 2005;**11**:2997-3004. DOI: 10.1002/chem.200401248
- [54] Hwang YK, Lee KC, Kwon YU. Nanoparticle routes to mesoporous titania thin films. *Chemical Communications*. 2001;**0**:1738-1739. DOI: 10.1039/B104699N
- [55] Angelome PC, Aldabe-Bilmes S, Calvo ME, Crepaldi EL, Grosso D, Sanchez C, Soler-Illia GJAA. Hybrid non-silica mesoporous thin films *New Journal of Chemistry*. 2005;**29**:59-63. DOI:10.1039/B415324C
- [56] Koganti VR, Dunphy D, Gowrishankar V, McGehee MD, Li XF, Wang J, Rankin SE. Generalized coating route to silica and titania films with orthogonally tilted cylindrical nanopore arrays. *Nano Letters*. 2006;**6**(11):2567-2570. DOI: 10.1021/nl061992v
- [57] Hayward RC, Alberius PCA, Kramer EJ, Chmelka BF. Thin films of bicontinuous cubic mesostructured silica templated by a nonionic surfactant. *Langmuir*. 2004;**20**(14):5998-6004. DOI: 10.1021/la030442z
- [58] Yamauchi Y, Sawada M, Sugiyama A, Osaka T, Sakka Y, Kuroda K. Magnetically induced orientation of mesochannels in 2D-hexagonal mesoporous silica films. *Journal of Materials Chemistry*. 2006;**16**:3693-3700. DOI: 10.1039/B608780A
- [59] Bass JD, Grosso D, Boissière C, Sanchez C. Pyrolysis, crystallization, and sintering of mesostructured titania thin films assessed by in situ thermal ellipsometry. *Journal of the American Chemical Society*. 2008;**130**(25):7882-7897. DOI: 10.1021/ja078140x

- [60] Fan Q, McQuillin B, Ray AK, Turner ML, Seddon AB. High density non-porous anatase titania thin films for device applications. *Journal of Physics D: Applied Physics*. 2000;**33**:2683-2686. DOI: 10.1088/0022-3727/33/21/303
- [61] Di Paola A, Bellardita M, Palmisano L. Brookite, the least known TiO<sub>2</sub> photocatalyst. *Catalysts*. 2013;**3**(1):36-73. DOI: 10.3390/catal3010036
- [62] Alberius PC, Frindell KL, Hayward RC, Kramer EJ, Stucky GD, Chmelka BF. General predictive syntheses of cubic, hexagonal and lamellar silica and titania mesostructured thin films. *Chemistry of Materials*. 2002;**14**:3284-3294. DOI: 10.1021/cm011209u
- [63] Mills A, Wang J. Simultaneous monitoring of the destruction of stearic acid and generation of carbon dioxide by self-cleaning semiconductor photocatalytic films. *Journal of Photochemistry and Photobiology A: Chemistry*. 2006;**182**(2):181-186. DOI: org/10.1016/j.jphotochem.2006.02.010
- [64] Wang K, Yao B, Morris MA, Holmes JD. Supercritical Fluid Processing of Thermally Stable Mesoporous Titania Thin Films with Enhanced Photocatalytic Activity. *Chemistry of Materials*. 2005;**17**(19):4825-4831. DOI: 10.1021/cm0508571
- [65] Mastropietro TF, Meringolo C, Poerio T, Scarpelli F, Godbert N, Di Profio G, Fontananova E. Multistimuli activation of TiO<sub>2</sub>/α-alumina membranes for degradation of methylene blue. *Industrial and Engineering Chemistry Research*. 2017;**56**(39):11049-11057. DOI: 10.1021/acs.iecr.7b02778
- [66] Machado AEH, Borges KA, Silva TA, Santos LM, Borges MF, Machado WA, Caixeta BP, França MD, Oliveira SM, Trovó AG, Patrocínio AOT. Applications of mesoporous ordered semiconductor materials — case study of TiO<sub>2</sub>. Ms. Bello SR. editor, *Solar Radiation Applications*, INTECH; 2015, DOI: 10.5772/59602
- [67] Banerjee S, Dionysiou DD, Pillai SC. Self-cleaning applications of TiO<sub>2</sub> by photo-induced hydrophilicity and photocatalysis. *Applied Catalysis B: Environmental*. 2015;**176**: 396-428. DOI: org/10.1016/j.apcatb.2015.03.058
- [68] Bai J, Zhou B. Titanium dioxide nanomaterials for sensor applications. *Chemical Reviews*. 2014;**114**(19):10131-10176. DOI: 10.1021/cr400625j
- [69] Mura S, Greppi G, Marongiu ML, Roggero PP, Ravindranath SP, Mauer LJ, Schibeci N, Perria F, Piccinini M, Innocenzi P, Irudayaraj J. FTIR nanobiosensors for *Escherichia coli* detection. *Beilstein Journal of Nanotechnology*. 2012;**3**:485-492. DOI: 10.3762/bjnano.3.55
- [70] Chen JC, Tan YL, Li CM, Cheah YL, Luan D, Madhavi S, Chiang Boey FY, Archer LA, Lou XW. Constructing hierarchical spheres from large ultrathin anatase TiO<sub>2</sub> nanosheets with nearly 100% exposed (001) facets for fast reversible lithium storage. *Journal of the American Chemical Society*. 2010;**132**(17):6124-6130. DOI: 10.1021/ja100102y
- [71] Liu Y, Yang Y. Recent progress of TiO<sub>2</sub>-based anodes for Li ion batteries. *Journal of Nanomaterials*. 2016, Article ID 8123652, 15 pages. DOI: 10.1155/2016/8123652
- [72] Zhang Y, Tang Y, Li W, Chen X. Nanostructured TiO<sub>2</sub> based anode materials for high-performance rechargeable lithium-ion batteries. *Chemistry of Nanomaterials for Energy, biology and more*. 2016;**2**(8):764-775. DOI: 10.1002/cnma.201600093

- [73] Fang H-T, Liu M, Wang D-W, Sun T, Guan D-S, Li F, Zhou J, Sham T-K, Cheng H-M. Comparison of the rate capability of nanostructured amorphous and anatase  $\text{TiO}_2$  for lithium insertion using anodic  $\text{TiO}_2$  nanotube arrays. *Nanotechnology*. 2009;**20**(22):225701-225708. DOI: 10.1088/0957-4484/20/22/225701
- [74] Ortiz GF, Hanzu I, Djenizian T, Lavela P, Tirado JL, Knauth P. Alternative Li-ion battery electrode based on self-organized titania nanotubes. *Chemistry of Materials*. 2009; **21**(1):63-67. DOI: 10.1021/cm801670u
- [75] Wang K, Wei M, Morris MA, Zhou H, Holmes JD. Mesoporous titania nanotubes: Their preparation and application as electrode materials for rechargeable lithium batteries. *Advanced Materials*. 2007;**19**(19):3016-3020. DOI: 10.1002/adma.200602189
- [76] Su X, Wu QL, Zhan X, Wu J, Wei S, Guo Z. Advanced titania nanostructures and composites for lithium ion battery. *Journal of Materials Science*. 2012;**47**(6):2519-2534. DOI: 10.1007/s10853-011-5974-x
- [77] Ortiz GF, Berenguer-Murcia A, Cabello M, Cazorla-Amorós D, Tirado JL. Ordered mesoporous titanium oxide for thin film microbatteries with enhanced lithium storage. *Electrochimica Acta*. 2015;**166**:293-301. DOI: 10.1016/j.electacta.2015.03.034
- [78] Jang K-S, Song M-G, Cho S-H, Kim J-D. Using the effects of pH and moisture to synthesize highly organized mesoporous titania thin films. *Chemical Communications*. 2004;**13**:1514-1515. DOI: 10.1039/B404409F